Improved Obstacle Mitigation and Localization Accuracy in Narrowband Ultrasonic Localization Systems using RoBCUL Algorithm

Sebastian Haigh* *Student Member, IEEE*, Janusz Kulon* *Senior Member, IEEE,*
Adam Partlow[†], Paul Rogers[†], and Colin Gibson[†]

Abstract

This paper develops a method for mitigating the negative effects of obstacles in narrowband, time division multiple access (TDMA), ultrasonic localization systems. The method builds upon the robust Bayesian classifier for ultrasonic localization (RoBCUL) algorithm which utilizes an iteratively reweighted least squares (IRLS) scheme. This algorithm has the advantage of low computational cost but loses performance in the presence of obstacles. The improved version of the RoBCUL algorithm presented in this paper uses a statistical test applied after each iteration of the regression, using a weighted residual vector calculated from the weight matrix and residual vector. The technique was tested using experimental data with its performance being quantified by its ability to correctly classify all the signals received during a single TDMA cycle. The extended version performed significantly better in all obstacle scenarios than the original, correctly classifying 100% of TDMA cycles in the scenarios with no obstacles, 99.9% with one obstacle, and 98.7% with two obstacles.

I. Introduction

Ultrasonic localization systems are an attractive choice in 3-D indoor positioning applications. The hardware required is readily available at low cost. In addition, the low propagation speed of the signals allows for precise time of flight measurement [1-3] and high accuracy 3-D position estimation. While the specific configuration of these systems can vary, all of them share the common trait of having ultrasonic transducers in various positions which transmit and receive signals between themselves. The received data is used, along with known information about the system, such as the position of fixed transducers, to calculate the 3-D position of a transducer in an unknown location [4].

Solid objects in the space between the various transducers can obstruct the line of sight (LOS) transmission of signals. Furthermore, such objects can cause non-line of sight (NLOS) interference by providing a source of signal reflection and diffraction. The combination of blocked LOS signals and the presence

of NLOS signals poses a challenging situation to any localization algorithm. Methods that can be applied to overcome these challenges in ultrasonic applications can be split into three main categories: broadband techniques, geometric techniques and techniques based upon robust least squares.

A. *Broadband Techniques*

Broadband techniques, such as code division multiple access (CDMA), which labels transmitted signals with identifying codes, can be used to good effect in overcoming both NLOS interference and the effects of signal loss due to obstruction. Codes, such as Gold codes, can be embedded into ultrasonic signals using techniques such as direct sequence spread spectrum (DSSS) or binary phase shift keying (BPSK). The use of such schemes limits CDMA to systems that can transmit and receive broadband signals, such as those described in [5 - 7].

Commercially available broadband transducers are more expensive, require higher driving voltages and are generally more fragile than piezoelectric narrowband transducers. Due to these limitations there are many applications in which the use of narrowband piezoelectric transducers is desirable, despite the resulting loss of available signal bandwidth. Where bandwidth is limited due to hardware, the CDMA techniques discussed above can still be used but will result in much lower performance. BSPK can be seen being applied in narrowband systems in [8-9], however, the stated accuracy of this system is approximately 10 cm. Many applications require greater accuracy, such as the anatomical landmark localization system developed by the authors of this paper and described in [10].

Narrowband systems can use linear frequency chirp signals. Linear chirp signals can offer high accuracy when the frequency sweep is very broad [11 - 13], however when the bandwidth (B) to center frequency (ω_0) ratio ($B/\omega_0 << 1$) is low the accuracy can deteriorate when the signal-to-noise ratio (SNR) is low [14]. In addition to the SNR, accuracy is also heavily influenced by the time-bandwidth product (BT) as described in [14]. Increasing BT increases the achievable accuracy. The effect of both BT and SNR on ultrasonic ranging accuracy is described by the following Cramer-Rao expression for the lower bound of the mean-squared error [12, 14]:

$$\varepsilon_{MSE} \geq \frac{\pi}{BT\omega_0^2\text{SNR}}. \tag{1}$$

Where ε_{MSE} is the lower bound of the the mean-squared error, the burst length T is expressed in seconds while the bandwidth B and center frequency ω_0 are both expressed in radians per second (rad/s).

Linear chirps can aid in the reduction of the number of multipath signals that are detected, this can be achieved by alternating the direction of the linear frequency sweep between consecutive transmission channels. Using alternating chirp signals results in a reduction in multipath components due to reflection. The relative orthogonality of the two signal types reduces the chance of multipath NLOS components of a signal transmitted in TDMA block k being detected in block $k+1$, this same multipath signal would need to arrive in block $k+2$ in order risk detection. However, while such an approach can reduce the number of NLOS signals detected it will not completely eliminate NLOS effects in heavy multipath environments.

B. Geometric Techniques

In [15] a geometrical approach is taken for testing pairs of received signals, utilising a triangle inequality to filter outliers. The triangle inequality states that if two measurements are taken from two fixed beacons to the same third node, the difference between the two measurements cannot be greater than the distance between the two beacons. While this approach is fast and simple to implement it has drawbacks that make it unsuitable and less robust than competing methods.

These drawbacks include coarse granularity, with [16] pointing out that this method can fail in certain geometrical situations. Another major drawback is a lack of outlier identification; the technique can detect that there are outliers but cannot specify which measurements are the outliers.

C. Least Squares Techniques

Robust least squares techniques use information generated during regression, such as residuals, to determine how well each of the measurements fits with the rest of the data. This information is then used to take corrective action in limiting the effect of these measurements on the result.

Least trimmed squares (LTS) and least median squares (LMS) perform multiple regressions upon different subsets of the entire set of recorded measurements. The subset with the lowest overall regression error can be considered free of NLOS interference. While this technique is robust, it is computationally

expensive [17]. LTS and LMS techniques can use the Levenburg-Marquardt (LM) algorithm to generate estimated positions for the various subsets of recorded measurements. Tests can then be applied to the solutions generated from these subsets, such as speed of sound estimation, as used in [18], or a test based upon position dilution of precision and the time of flight measurement error variance, as used in [19].

In a previous paper[20] the authors presented the RoBCUL algorithm, a robust classifier using Bayesian probability and iteratively reweighted least squares. This technique exhibited excellent performance in identifying and rejecting reflected NLOS signals and did so with a substantial saving in computational cost over similar methods. However, there is a loss of performance when the line of sight paths between receiver-transmitter pairs are obstructed. For practical applications, such as the one outlined in [10], where the possibility of blocked signals is highly likely, it is essential to overcome the negative effects this can cause. The best available methods for doing this are the LTS and LMS techniques. However, these methods are computationally expensive, and it was due to this that the RoBCUL algorithm was originally developed in [20].

The main objective of this study was to investigate if the RoBCUL could be made robust to the effects of complete LOS signal blockage due to obstacles without compromising the computational cost benefits of the original algorithm. In addition, a new and extensive experimental work was conducted to study the effect of using alternating narrowband chirp signals on both LOS and NLOS signal classification and the 3-D positioning error within the new version of RoBCUL algorithm.

The basic concept of mitigating the effect of obstacles using RoBCUL algorithm was first reported at the 2019 IEEE International Instrumentation and Measurement Technology Conference [21]. Preliminary experimental results were presented using single frequency ultrasonic bursts of 32.8 kHz. This paper presents in detail the improvement to the original RoBCUL algorithm consisting of an additional weighting procedure, which significantly increases the performance of the algorithm in the presence of LOS obstructions, while only requiring a small increase in the computational complexity of the the algorithm. The experimental validation of the extended algorithm was carried out using alternating linear chirps instead of single frequency ultrasonic bursts, leading to both increased positioning accuracy and multipath rejection characteristics even in a severe multipath environment with high attenuation of the signals.

Section II will detail the improvements that have been made to the RoBCUL algorithm, sections III

and IV detail the experimental work that was carried out to test the improvements and the results of that testing, with a discussion of the results and performance of the improvements in section V.

II. IMPROVED RoBCUL ALGORITHM FOR MITIGATION OF COMPLETE LOS BLOCKAGE

This section will present an additional weighting procedure, shown in Fig. 1, for the RoBCUL algorithm that increases performance in situations where LOS signal blockage occurs due to the presence of obstacles.

A. Overview of the Original RoBCUL Algorithm

In [20] the terms block and frame were defined to refer to specific windows of the received signal timeseries. A block is defined as the window of this timeseries from the sample at which one transmitter begins its transmission to the sample immediately before the next transmitter begins its transmission. A frame is defined as the window of the timeseries which contains all the blocks for a single TDMA cycle.

The RoBCUL algorithm calculates the probability of a signal being LOS using the signals amplitude and a pair of Gaussian probability density functions for the amplitude of LOS and NLOS signals, $p(s_i|A)$ and $p(s_i|A^*)$ respectively.

These probability density functions can be generated from data collected during calibration tests before the system is used. Once the system is set up in a space, receivers can be placed in known positions and signals can be sent from each transmitter. If both the transmitter and receiver positions are known, then the exact length of each LOS path can be calculated using basic geometry. If the LOS path distances are known, then the LOS and NLOS signals can be found easily in the received data. Once this data is collected, the mean and standard deviation can be calculated for each data set and this information used to parametrise the required probability density functions.

The classification itself uses an iteratively reweighted regression working on the signals received during a single frame. Starting from an initial guess of the coordinates, held in a vector of parameters $\mathbf{x} = [x, y, z]^T$. This regression uses the LM algorithm to calculate parameter updates. During each iteration a custom weight update rule is implemented that changes the weights of each of the signals depending on the current residual of the signal and its previously calculated probability.

The weighted update equation for the LM algorithm is shown in (2), and the weight update rule is shown in (4)

$$\mathbf{x}_{i+1} = \mathbf{x}_i - (\mathbf{J}^T\mathbf{W}\mathbf{J} + \lambda\mathrm{diag}(\mathbf{J}^T\mathbf{W}\mathbf{J}))^{-1}\mathbf{J}^T\mathbf{W}\mathbf{r}(\mathbf{x}), \tag{2}$$

where $\mathbf{J}$ is the Jacobian matrix of the residual equation with respect to the parameter vector, *i.e.*: $\mathbf{J} = \frac{\partial \mathbf{r}(\mathbf{x})}{\partial \mathbf{x}}$. $\mathbf{W}$ is a weight matrix, λ is the LM parameter and the elements of the residual vector, $\mathbf{r}(\mathbf{x})$, are given by:

$$r_{k|i}(\mathbf{x}) = d_{k|i} - \sqrt{(x - x_k)^2 - (y - y_k)^2 - (z - z_k)^2}, \tag{3}$$

where $d_{k|i}$ is the distance associated with the signal $s_{k|i}$ and x_k, y_k, z_k are the coordinates of the kth transmitter.

The weight update rule for each iteration is given as:

$$w_{k|i} = \begin{cases} \dfrac{\gamma}{|r_{k|i}|}\hat{\phi}_{k|i} & \text{if } |r_{k|i}| > \gamma \\ 1 & \text{else}, \end{cases} \tag{4}$$

where $w_{k|i}$ is the weight of signal $s_{k|i}$, γ is a threshold value related to the error of the range measurements [20], and probability of the signal $s_{k|i}$ being LOS is given by $\hat{\phi}_{k|i}$, which can be calculated using (5) and (6):

$$\hat{\phi}_{k|i}^- = p(A|s_i) = \frac{p(s_i|A)p(A)}{p(s_i|A)p(A) + p(s_i|A^*)p(A^*)}, \tag{5}$$

$$\hat{\phi}_{k|i} = \frac{\hat{\phi}_{k|i}^- p(s_i)}{\sum_{j=1}^n \hat{\phi}_{k|j}^- p(s_j)}. \tag{6}$$

By iteratively updating the weight of each signal in this manner, the weights of LOS signals converge to a value near one (giving them a large influence over the value of the parameter estimate) and the weights of the NLOS signals converge to near zero giving them very little influence. Any given block can contain a single, multiple or no NLOS signals, it can also either contain zero or one LOS signals.

The original RoBCUL algorithm exhibits excellent performance when there is one LOS signal in every block. This performance worsens, however, if this condition is not met. Obstructed LOS paths result in a loss of useful information for estimating the position of the receiver. Furthermore, obstructed LOS paths also result in NLOS signals representing a higher percentage of all the received signals. The fast convergence method of the original algorithm as outlined in [20] will increase the weight of the lowest residual signal which, when a high percentage of all signals are NLOS, is more likely to be an NLOS signal. This method is still required in order to stop the algorithm from taking a long time to converge, therefore removing this method will not increase the performance of the algorithm in any scenario.

In a situation where there are too many NLOS signals and not enough LOS information for the original RoBCUL algorithm to be capable of finding a solution, another method is required of filtering out NLOS signals. An additional NLOS filter will allow for the ratio of LOS to NLOS signals to be improved, creating a situation in which the algorithm can find a solution.

B. New Fault Detection & Exclusion Procedure

A fast fault detection procedure has been developed for the RoBCUL algorithm as an extension of the existing weight update. This procedure is designed to estimate the leverage that each received signal has on the regression without resorting to highly computationally expensive techniques. At the end of each iteration, each signal in the regression will have a weight and a residual. The current weight of each signal reflects how likely that signal is to be a LOS signal, while the residual reveals how well this signal fits with the current estimate of the position. If the current estimate of the position is not too far from the true position then the LOS signals will have the lowest residuals of all the signals, while any NLOS signals will have higher residuals. Weights in the range $0 \leq w \leq 1$ are assigned to each signal, with 0 being least likely and 1 being most likely. Therefore, correctly classified LOS signals will have a weight of near one and a residual near to zero, and a signal that is correctly classified as NLOS will have a weight near zero
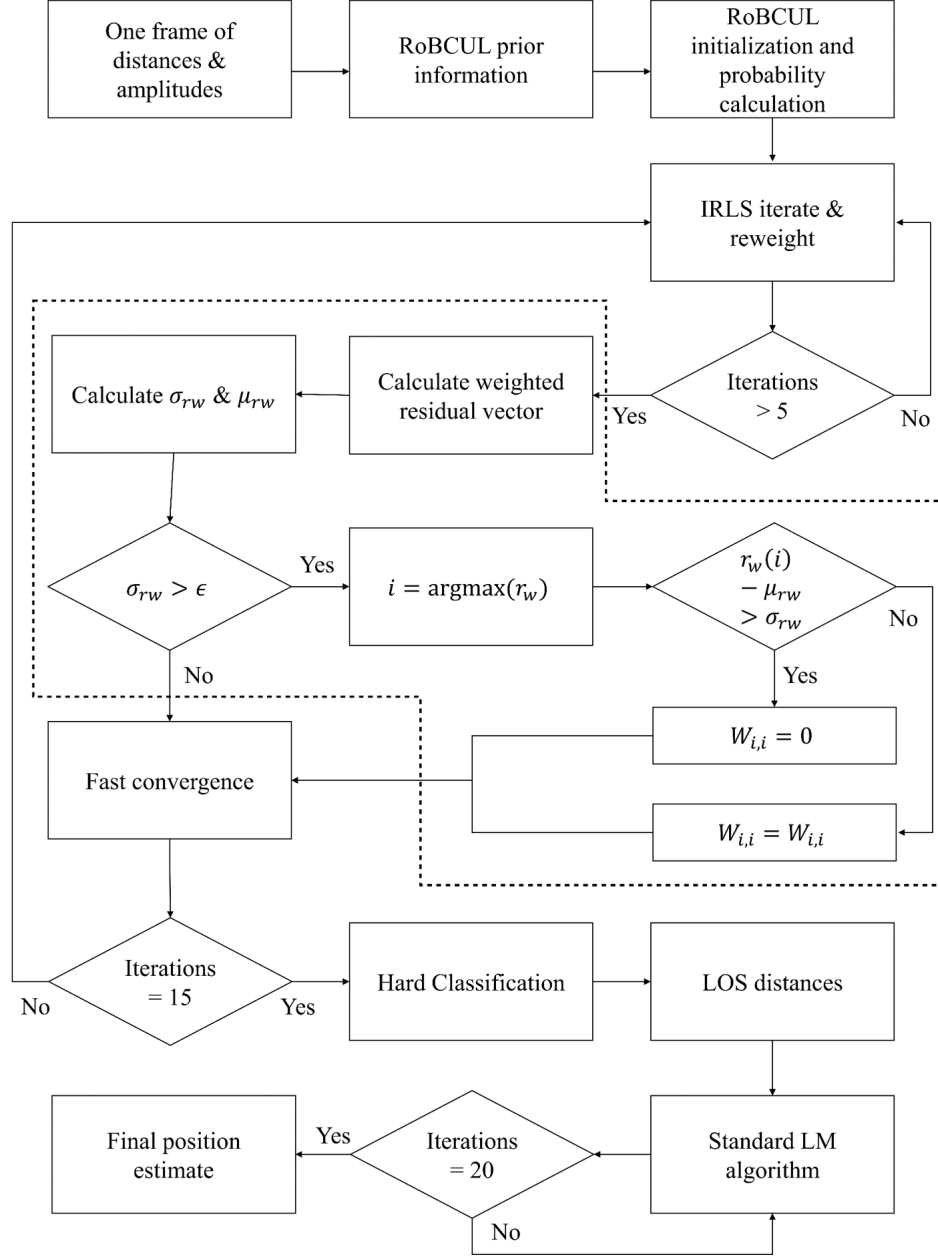
Fig. 1. Flowchart showing the functioning of the algorithm extension within the original algorithm. The blocks within the dashed lines represent additions to the algorithm made in this paper. The new procedure takes place after the original weight update step, the $\mathbf{r_w}$ vector is calculated along with its standard deviation (σ_{rw}) and mean (μ_{rw}). If σ_{rw} does not exceed the value of the threshold ϵ then the algorithm continues along its original path. If $\sigma_{rw} > \epsilon$ then the new fault detection and exclusion step is triggered, eliminating the signal with the highest weighted residual if that signals weighted residual is more than σ_{rw} from μ_{rw}.

and a high value residual.

A second situation is possible where the current position estimate is not close to the true position. In such a situation, all of the residuals of the signals will likely be high and therefore the original algorithm will have given each signal a low weight. This situation is likely where there has been LOS path blockage and, as a result, the number of NLOS signals is greater than the number of LOS signals. This can cause the algorithm to become unable to converge, since there are too many NLOS outliers compared to LOS signals. In such a situation this method will remove the signals that are most likely to be NLOS from the regression. This will allow the mechanisms provided by the original algorithm to find a solution, by increasing the percentage of LOS signals.

To detect faulty classifications, the weight matrix $\mathbf{W}$ can be multiplied by the absolute value of the residual vector $\mathbf{r}(\mathbf{x})$, resulting in a weighted-residual vector $\mathbf{r_W}$, with each of the elements of the vector corresponding, in order, to each of the signals. The absolute value is used because only the magnitude of weighted-residuals is important in detecting faulty classifications,

$$\mathbf{r_W} = |\mathbf{W}\mathbf{r}(\mathbf{x})|. \tag{7}$$

Since a false LOS signal is an NLOS signal with a weight near one, the element of $\mathbf{r_W}$ corresponding to such a signal will be large, whereas correctly classified signals will all have small weighted-residual values, either LOS signals with near unity weights and small residuals or NLOS signals with large residuals and near zero weights. Thus, false LOS signals will be easy to detect in $\mathbf{r_W}$ due to the large magnitude of their weighted-residuals. False NLOS will be undetected by this method since these signals will have both small residuals and near zero weights, however such signals can be dealt with by the existing reweighting procedure which will detect the low residual and assign a higher weight.

Once the weighted-residual vector has been calculated, in order to identify and exclude incorrect classifications the standard deviation (σ_{rw}) of $\mathbf{r_W}$ is estimated using the root mean squared error ($RSME$):

$$\sigma_{rw} = \sqrt{\frac{1}{N} \sum_{i=1}^{N} r_W^2[i]}. \tag{8}$$

The mean (μ_{rw}) of the weighted-residual vector is also calculated. If all signals have been correctly classified both values should be small and consistent with the expected measurement error of the range measurements. The known value of the standard deviation of the measurement error is defined as ε. If the standard deviation of the absolute values of the weighted-residual vector is less than ε no corrective action will be taken, and it will be assumed that the signals have been correctly classified.

If $\sigma_{rw} > \varepsilon$ it will be assumed that there is at least one incorrect classification and corrective action will be taken. At each iteration, the algorithm is given the chance to exclude a single signal, therefore the signal with the greatest weighted-residual will be considered. If this signal's weighted-residual is more than one standard deviation above the mean, then the signal will be rejected. The rejection is performed by setting the weight of the signal to zero.

If the maximum weighted-residual is the ith element in the weighted-residual vector, then:

$$\mathbf{W}_{i,i} = \begin{cases} 0 & \text{if } \mathbf{r_W}(i) - \mu_{rw} > \sigma_{rw} \\ \mathbf{W}_{i,i} & \text{if } \mathbf{r_W}(i) - \mu_{rw} \leq \sigma_{rw}. \end{cases} \tag{9}$$

That is, the corresponding weight will be set to zero if the ith weighted-residual is more than one standard deviation above the mean and will be unchanged otherwise. This process will be repeated during the iterations that follow until either the maximum number of iterations is reached or until there are only three signals left with non-zero weights.

The value of ε is chosen as the standard deviation of the measurement error since if all the signals are correctly classified, then the values that will dominate the weighted residual vector will be the residuals of the LOS signals. The error of these signals will therefore conform to the standard deviation of the measurement error for LOS signals. If there are NLOS signals classified as LOS signals then the standard deviation of the weighted-residual vector will be above that of the measurement error of LOS signals.

C. Computational Complexity

In [20] the computational complexity of the algorithm was estimated by considering the number of multiplications required per iteration of the algorithm. For the original algorithm [20] gives this value as:

$$M_O = 3a^2 + 12a + 27, \tag{10}$$

where M_O is the number of multiplications for the original algorithm and a is the number of LOS and NLOS signals that have been received.

The new weighting procedure presented in this paper requires additional multiplications and therefore $M_E > M_O$, where M_E is the number of multiplications required for the extended version of the algorithm. The new procedure requires that the weight matrix $\mathbf{W}$ be multiplied by the residual vector $\mathbf{r}(\mathbf{x})$. Since $\mathbf{W}$ is a diagonal matrix and $\mathbf{r}(\mathbf{x})$ is a column vector, this is achieved by a simple element-wise multiplication. If the number of signals in the regression is a then $\mathbf{W}$ is an $a \times a$ matrix and $\mathbf{r}(\mathbf{x})$ is an $a \times 1$ vector, the weighted residual vector $\mathbf{r_W}$ will also be an $a \times 1$ vector with elements $r_{wi} = W_{i,i}r_i$, this can be performed with a multiplications.

Likewise squaring each element of $\mathbf{r_W}$ in the estimation of σ_{rw} will take a multiplications. Both the calculation of σ_{rw} and μ_{rw} require one division, giving

$$M_E = 3a^2 + 15a + 29, \tag{11}$$

per iteration, which is not a significant increase in the computational complexity.

III. EXPERIMENTAL TESTING

To test the proposed technique data was collected from a series of experiments. These experiments used eight transmitters held in two perpendicular planes and cylindrical pipes to act as obstacles.

When it is likely that the LOS path of multiple signals may be blocked by obstacles, it is prudent to

add more transmitters to the system. Since the hardware used by narrowband ultrasonic systems is cheap, this is often the simplest and best course of action. However, with the addition of more transmitters, the likelihood of multipath interference and destructive interference increases. Also, when increasing the number of transmitters, the number of received NLOS signals will likewise increase and the need for efficient and robust algorithms to detect and reject outliers remains.

A rig was designed and constructed for holding the transmitters and receivers in known locations during the experiment. The rig had two transmitter arrays, each of which held four transmitters, with each transmitter being positioned at the vertex of a square. These arrays were positioned such that transmitter planes one and two were parallel to the t_1 and t_2 axes respectively. As shown in Fig. 2 the t_1 and t_2 axes are rotations of the x and y axes.

A receiver array was constructed and placed upon a linear rail, allowing it to be moved though the space in front of the transmitters. The receiver array was positioned at a 45° angle to both transmitter arrays. Receiver positions on the array were spaced 100 mm in both the vertical and horizontal directions. The receiver array allowed for receivers to be held in any of 30 different positions within the plane of the array, and the linear rail mounting allowed the array to be positioned anywhere along an 800 mm track. During the experiment, intervals of 100 mm were used to position the receiver array. This allowed for eight different rail positions and a total of 240 possible receiver positions. Three microphones were used as the receivers in the experiment, and were repositioned between test runs in order to cover the entire space.

To investigate the effects of obstacles, cylindrical objects were placed in various positions between the transmitters and receivers. These cylinders, formed of hollow PVC ducting, were 150 mm in diameter and 1500 mm in height. The hard plastic surface of the obstacles presents a highly acoustically reflective surface which further increases the environmental interference.

A full set of experiments was run with one and two obstacles as well as a full set run with no obstacles. During the experiments with obstacles, the obstacles were held in one of three positions (P1, P2, and P3) as shown in Fig. 2. All obstacles were placed 400 mm from the transmitter arrays as shown in Fig. 2. If one obstacle was used, this obstacle would be placed in front of transmitter plane 2. If two obstacles were used then one would be placed in front of each of the transmitter planes.
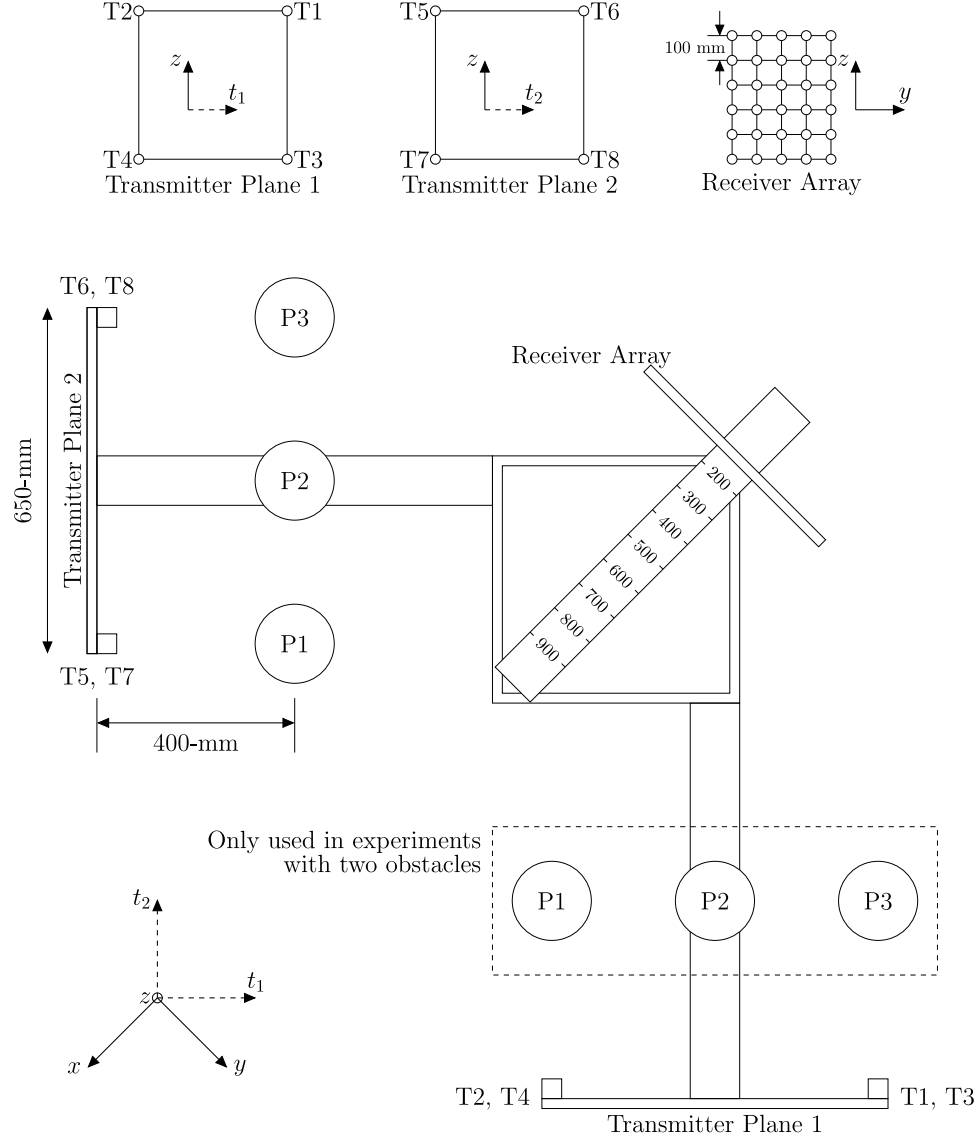
Fig. 2. Experimental rig layout showing obstacle positioning. There are six possible configurations of obstacle position shown, three with one obstacle and three with two obstacles. Either there is obstacle in the P1, P2, or P3 position in front of transmitter two, or there are two obstacles where both are in the P1, P2, or P3 position, with one in front of Transmitter Plane 1 and one in front of transmitter plane 2. At the top of the figure the layout of the individual transmitters is shown in each arrays own plane.

While there exist other combinations of obstacle number and position that could have been explored, the combinations that were used were chosen as they result in a wide range of LOS blockage and NLOS multipath effects throughout the space containing the receivers.

A. Ultrasonic Signals

Each run consisted of sending 30 ultrasonic bursts from each transmitter. Each ultrasonic burst was a linear chirp, with a center frequency of 40 kHz, bandwidth of 4 kHz and length of 5 ms. Input and output

sampling was performed at 754,717 Hz. Each run was repeated three times.

A linear chirp is a sine wave with an instantaneous frequency $f(t)$ that varies linearly with respect to time. Such a signal $S_i(t)$ is described by

$$S_i(t) = \text{rect}\left(\frac{t}{T}\right) \sin\left[2\pi \left(\frac{u_i}{2}t^2 + f_{si}\right) + \psi\right], 0 < t < T, \tag{12}$$

where $\text{rect}(\cdot)$ is the rectangular window function, t is time in seconds, T is length of the burst in seconds, ψ is phase and u_i is given by

$$u_i = \frac{f_{ei} - f_{si}}{T}, \tag{13}$$

where f_{si} and f_{ei} are the starting and ending frequencies of the ith waveform, respectively. In our system we have two signals, $S_1(t)$ and $S_2(t)$ with frequencies: $f_{s1} = 38$ kHz, $f_{e1} = 42$ kHz and $f_{s2} = 42$ kHz, $f_{e2} = 38$ kHz.

With a bandwidth of 4 kHz (25,132 rad/s), burst length of 5 ms, center frequency of 40 kHz (251,327 rad/s) and assuming an SNR of 1, using (1): $\varepsilon_{MSE} \geq 3.958 \times 10^{-13}$ s.

While multipath signals are reduced by the use of such signals, NLOS components in the form of diffracted signals remain, and are common in environments with obstacles. Diffraction allows accoustic signals to travel around obstacles that block the LOS transmission path, arriving at the receiver having travelled an NLOS path, with the resulting error in time of flight. The amplitude of such a signal, as well as the magnitude of the correlation peak associated with it will be less than that of an equivalent LOS signal. However, due to attenuation induced by the directionally of the transmitters, the amplitude alone is an ambiguous indicator of NLOS signals.

Theoretically, it is advantageous to maximise the bandwidth and the burst length; increasing either or both of these quantities also increases time-bandwidth product, which has a significant effect on the Cramér-Rao lower bound for mean-square error of the distance measurements [14]. However, there are several practical considerations that must be taken into account when selecting these signal characteristics.

The bandwidth is limited by the hardware of the system. The value of 4 kHz was chosen as it is the widest bandwidth possible with the transmitters used. The burst length is limited by the amount of time that can be dedicated to each channel. Since we use a TDMA scheme here, increasing the length of the bursts requires an increase in the length the time blocks that are assigned to each transmitting channel. The value of 5 ms was chosen as this ensures that the component of uncertainty that is due to the time-bandwidth product is much less than other sources of error, while also allowing the TDMA block for each channel to be less than 8 ms.

The transmitters used were Murata MA40S4S piezoelectric transducers and the receivers were Knowles FG-23329-P07 electret microphones. The Murata MA40S4S has center frequency of 40 kHz, at which it outputs 120 dB sound pressure level (SPL), furthermore this transducer outputs 110 dB SPL or greater in the frequency range of 38 kHz to 42 kHz.

The received signal was amplified using an Alligator Technologies USBPIA-S1 programmable instrumentation amplifier with a gain of five. A National Instruments USB-7856R Multifunction RIO device was used for input and output sampling, this device is capable of simultaneous input and output sampling of up to 1 MHz on 8 output channels and 4 differential input channels.

B. Pre-Processing of Experimental Data

The data collected during the experiments was a timeseries of the digitized voltages recorded by the receiver. The input to the RoBCUL algorithm and its extended version are distances and amplitudes. It is therefore necessary to process the data received in order to obtain these distances and amplitudes.

The received timeseries was cross-correlated with stored reference copies of the transmitted signals $S_1(t)$ and $S_2(t)$. The result of this correlation is a third signal containing sharp peaks, with maximums at the time of arrival of the various received LOS and NLOS ultrasonic bursts. The distance travelled can be calculated from the time of flight using:

$$d = c_H(n_a - n_{b0})T_s, \tag{14}$$

where n_a is the sample at which the signal arrived, n_{b0} is the start sample of the TDMA block b, T_s is the sampling period, and c_H is the temperature and humidity compensated speed of sound which can be calculated from the temperature compensated speed of sound c_T, the air temperature T_C and relative humidity h_r using (15) [22]

$$
\begin{aligned}
c_T &= 20.05\sqrt{T_C + 273.16}\,\text{ms}^{-1} \\
c_H &= c_T + h_r[1.0059 \times 10^{-3} \\
&+ 1.7776 \times 10^{-7}(T_C + 17.78)^3]\,\text{ms}^{-1}.
\end{aligned}
\tag{15}
$$

Once the arrival time of the bursts is known from the correlation, it is trivial to find the maximum amplitude of that burst from the received data. The result of the above processes will be a vector of distances $\mathbf{d} = [d_1, d_2, \ldots, d_N]^T$ and a vector of amplitudes $\mathbf{a} = [a_1, a_2, \ldots, a_N]^T$, which are the required inputs to the RoBCUL algorithm.

IV. EXPERIMENTAL RESULTS

Results are presented here from testing the proposed algorithm on the data collected during the experiment. The classification results are shown in the bar charts in Fig. 4. These charts show the percentage of TDMA frames in which the algorithm was capable of correctly classifying all the signals, if even one signal in a frame is incorrectly classified then the frame is counted as a failure. The charts are broken down by the position of the receiver array on its linear rail support. Table I presents the minimum, maximum and mean average values from each chart in Fig. 4. Cumulative error plots shown in Fig. 3 are used to present the 3-D positioning accuracy of the localization, where the 3-D positioning error is defined as the Euclidean distance between the known position of the receiver $\mathbf{x}_r = [x_r, y_r, z_r]^T$ and the position estimated by the algorithm $\hat{\mathbf{x}} = [\hat{x}, \hat{y}, \hat{z}]^T$. The 3-D positioning error e_{3D} is therefore:

$$
e_{3D} = \sqrt{(x_r - \hat{x})^2 + (y_r - \hat{y})^2 + (z_r - \hat{z})^2}
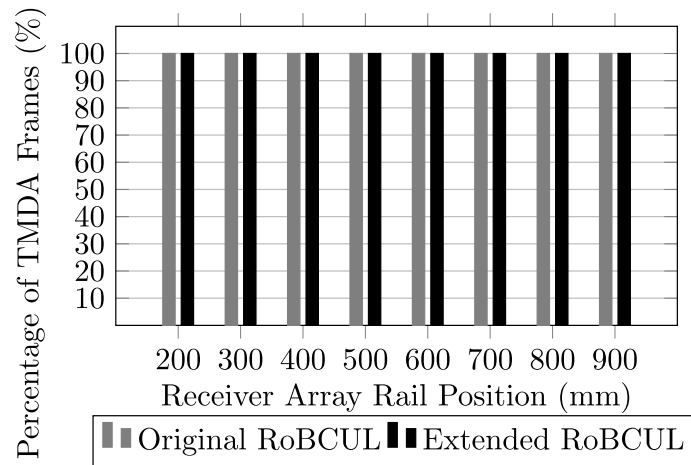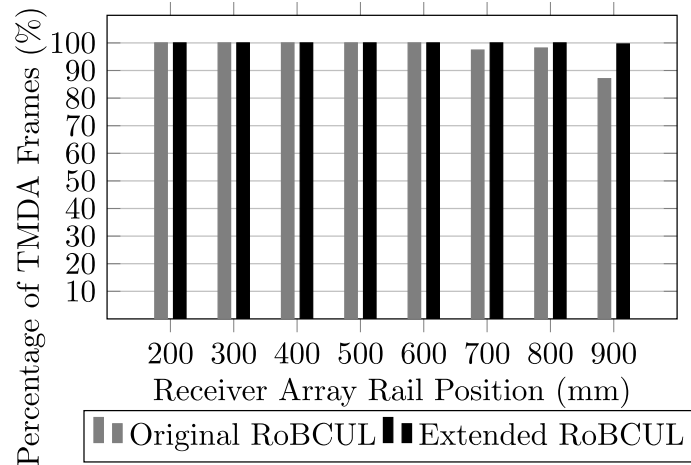\tag{16}
$$
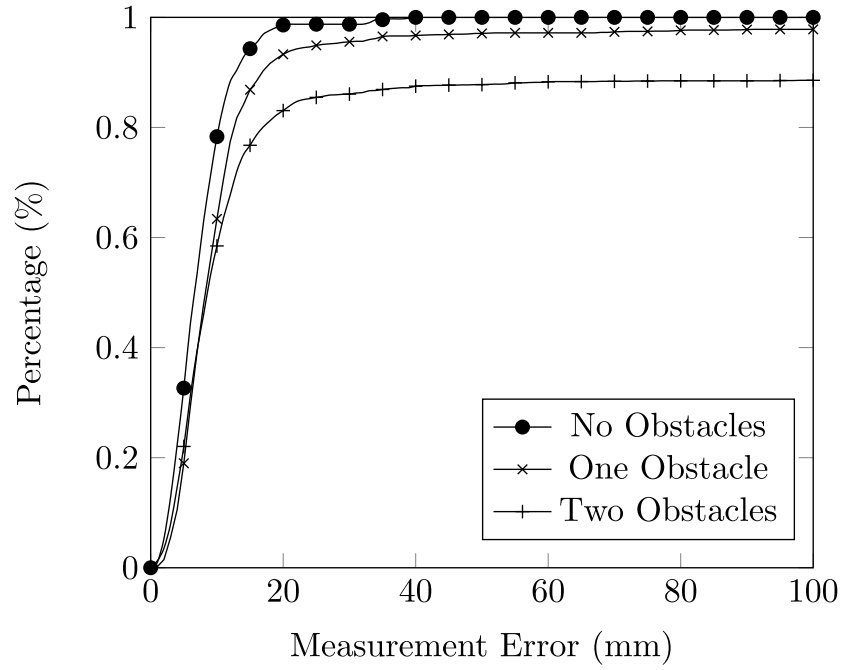
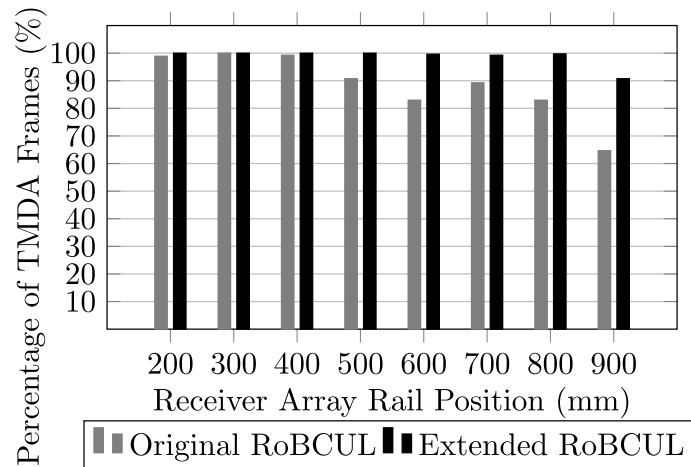(a) Original RoBCUL
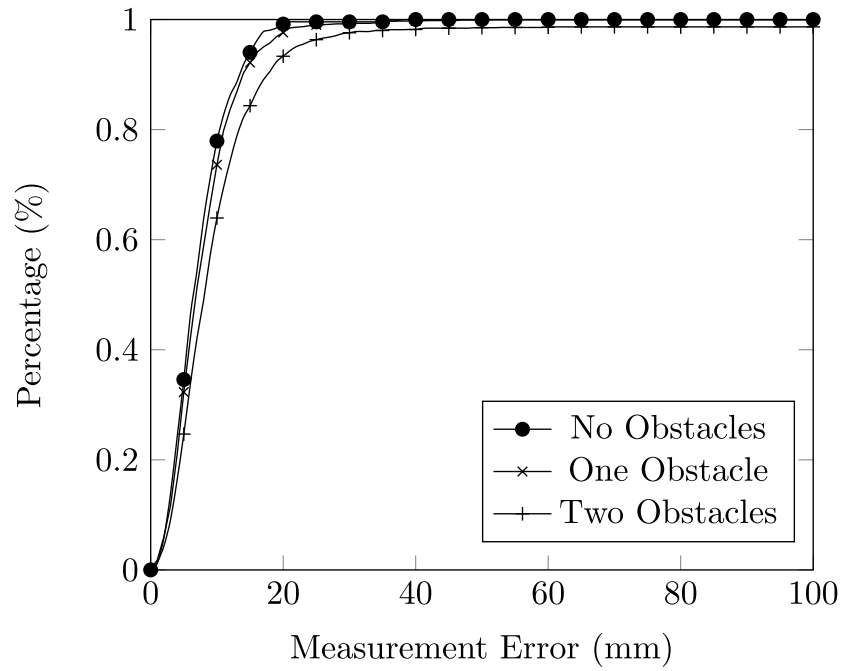
(b) Extended RoBCUL

Fig. 3. Cumulative error plots of the 3-D positioning error, as defined in (16), for (a) the original RoBCUL algorithm as described in **Haigh2019** and (b) the extended RoBCUL algorithm as described in this paper. Tick marks are every 5 mm.

(a) Classification Performance, No Obstacles

(b) Classification Performance, One Obstacle

(c) Classification Performance, Two Obstacles

Fig. 4. Bar charts showing a comparison of classification performance of the original and extended versions of the RoBCUL algorithm in (a) experiments with no obstacles, (b) experiments with one obstacle, and (c) experiments with two obstacles. In each case results are broken down by the position of the receiver array on its linear guide rail as shown in figure 2. The minimum, maximum and mean of these results are summarized in Table I.

TABLE I

COMPARISON OF THE PERFORMANCE OF THE ORIGINAL AND EXTENDED ROBCUL ALGORITHM. MINIMUM, MAXIMUM, AND MEAN
CLASSIFICATION RESULTS IN THE PRESENCE OF ONE, TWO OR NO OBSTACLES, FOR ALL EXPERIMENTS.

Algorithm	No. of Obs.	Min. (%)	Max. (%)	Mean (%)
Original	Zero	100	100	100
Original	One	87.1	100	91.8
Original	Two	64.7	100	88.6
Extended	Zero	100	100	100
Extended	One	99.6	100	99.9
Extended	Two	90.7	100	98.7

V. DISCUSSION

The results shown in Fig. 3 and Fig. 4 demonstrate the performance of the proposed method. As would be expected, the best results are obtained in the experiments without obstacles and the worst are found in the experiments with two obstacles.

A. Classification

The data in Fig. 4 and Table I show that the extended algorithm, on average, correctly classified 8.1% more frames with one obstacle, and shows the greatest increase in performance when two obstacles are present, with an 10.1% increase in the number of correctly classified frames. There was no change in the results for experiments without obstacles, with both algorithms correctly classifying 100% of frames.

The greatest increases in performance were in the experiments where the receiver array was in the 900 mm rail position. In this position, and with two obstacles, the use of the extended algorithm resulted in a 26.1% increase in the number of correctly classified frames.

A trend can be seen in Fig. 4c of a significant deterioration in performance of the original algorithm when the receiver array was moved beyond the 500 mm mark. The performance gets progressively worse as the receiver array was moved further, with the 900 mm position presenting the worst results with two obstacles, for both algorithms, with this position being the only scenario tested in which the classification accuracy of the extended algorithm drops below 99%.

In these experiments the 900 mm position was the worst receiver position with respect to LOS coverage when the two obstacles were in position P1, completely obstructing the LOS path between the receivers and transmitters T2, T4, T5, and T7. Only transmitters T1, T3, T6, and T8 had a clear line of sight connection to the receiver plane. However, with the receivers in this position, the LOS path was at an average angle of 40° from the central axis of the LOS transmitters. Due to the narrow beam angle of the transmitters, this transmission angle resulted in approximately -6 dB attenuation from the maximum sound pressure level. Therefore, the LOS signals that were reaching the receiver from these positions were highly attenuated.

This increased signal attenuation degrades the classification performance of the original RoBCUL algorithm, even in the cases where there are no obstacles to obstruct the signals. This is due to the fact that high attenuation of the LOS signals increases the likelihood of only a NLOS signal being detected in the effected blocks. Due to the requirement of the original RoBCUL algorithm, that there should be one LOS signal present in every block, this situation causes the original algorithm to fail, as the single NLOS signal is often misconstrued to be LOS. However, with the additional step presented in this paper the extended algorithm can greatly diminish this effect in all cases.

B. Positioning Accuracy

The benefit of the use of chirp signals allows for greater accuracy than was achieved with the use of single frequency signals in [20, 21]. Fig. 3 shows that the algorithm increases the accuracy of the system, by eliminating outlying range measurements. It can be seen in Fig. 3b that using the additional weighting procedure outlined in this paper 78.9% estimated positions had an error of less than 10 mm in the experiments with no obstacles. For the experiments with one and two obstacles, the percentage of estimated positions with errors less than 10 mm was 73.6% and 63.9% respectively.

Furthermore, 99.2% (no obstacles), 97.6% (one obstacle), and 93.3% (two obstacles) of errors are less than 20 mm. This can be compared to the results obtained by the original algorithm of 98.6% (no obstacles), 93.3% (one obstacle), and 83.1% (two obstacles).

The receivers used have good omni-directionality presenting minimal attenuation even at the wide angles experienced in the the 700 mm to 900 mm range. However, the transducers have a narrow beam angle

and therefore some attenuation is experienced when the LOS path between the transmitter and receiver is at a wide angle from the transmitter central axis. The reduction in amplitude of the signal with no change in the noise level leads to a decrease in the SNR. As discussed in [14] the achievable accuracy of narrowband chirp signals is sensitive to the SNR.

VI. CONCLUSION

A method for mitigating the effects of obstructions in narrowband ultrasonic localization systems has developed and presented, this method extends the RoBCUL algorithm presented in [20].

The extended algorithm uses a weighted-residual vector, and a statistical test applied to the elements of that vector, at each iteration to detect NLOS signals that have been incorrectly classified as LOS. The extension not only gives the algorithm the ability to detect that there are faults, but also to determine which signals are faulty and to remove those signals.

The extended algorithm was tested on data collected during experiments which featured a number of obstacles in different positions. The extended algorithm performed comparably in the baseline, no obstacle case, with both algorithms correctly classifying 100% of frames. Furthermore, the proposed extended algorithm performed better than the original RoBCUL algorithm in both scenarios featuring obstructions. With one obstacle present the extended algorithm classified 99.9% of frames correctly (compared with 91.8% for the original algorithm). With two obstacles present the extended algorithm classified 98.7% of frames correctly (compared with 88.6% for the original algorithm).

The use of linear chirp signals in conjunction with the extended RoBCUL algorithm resulted in greater positioning accuracy compared to the original RoBCUL, with less than 1cm error for 78.9% measurements with no obstacles, and 73.6% and 63.9% for the experiments with one and two obstacles respectively, while maintaining superior classification accuracy.

REFERENCES

[1] G. Andria, F. Attivissimo, and N. Giaquinto, "Digital signal processing techniques for accurate ultrasonic sensor measurement," *Measurement: Journal of the International Measurement Confederation*, vol. 30, no. 2, pp. 105-114, 2001. DOI: 10.1016/S0263-2241(00)00059-2.
[2] M. Parrilla, J. Anaya, and C. Fritsch, "Digital signal processing techniques for high accuracy ultrasonic range measurements," *IEEE Transactions on Instrumentation and Measurement*, vol. 40, no. 4, pp. 759763, 1991. DOI: 10.1109/19.85348.

[3] D. Marioli, C. Narduzzi, C. Offelli, D. Petri, E. Sardini, and A. Taroni, "Digital Time-of-Flight Measurement for Ultrasonic Sensors," *IEEE Transactions on Instrumentation and Measurement*, vol. 41, no. 1, pp. 9397, 1992. DOI: 10.1109/19.126639.

[4] A. De Angelis, A. Moschitta, P. Carbone, M. Calderini, S. Neri, R. Borgna, and M. Peppucci, "Design and Characterization of a Portable Ultrasonic Indoor 3-D Positioning System," *IEEE Transactions on Instrumentation and Measurement*, vol. 64, no. 10, pp. 26162625, 2015. DOI: 10.1109/TIM.2015.2427892.

[5] M. Alloulah and M. Hazas, "An efficient CDMA core for indoor acoustic position sensing," in *2010 International Conference on Indoor Positioning and Indoor Navigation, IPIN 2010 - Conference Proceedings*, pp. 1517, 2010. DOI: 10.1109/IPIN.2010.5648279.

[6] N. M. Vallidis, "WHISPER: A Spread Spectrum Approach to Occlusion in Acoustic Tracking," PhD thesis, University of North Carolina, 2002.

[7] J. R. Gonzalez and C. J. Bleakley, "High-Precision robust broadband ultrasonic location and orientation estimation," *IEEE Journal on Selected Topics in Signal Processing*, vol. 3, no. 5, pp. 832844, 2009. DOI: 10.1109/JSTSP.2009.2027795.

[8] T. Aguilera, F. J. Alvarez, D. Gualda, J. M. Villadangos, A. Hernandez, and J. Urena, "Multipath Compensation Algorithm for TDMA-Based Ultrasonic Local Positioning Systems," *IEEE Transactions on Instrumentation and Measurement*, vol. 67, no. 5, pp. 984991, 2018. DOI: 10.1109/TIM.2018.2794939.

[9] J. A. Paredes, F. J. Alvarez, T. Aguilera, and J. M. Villadangos, "3D indoor positioning of UAVs with spread spectrum ultrasound and time-of-flight cameras," *Sensors (Switzerland)*, vol. 18, no. 1, pp. 115, 2018. DOI: 10.3390/s18010089.

[10] J. Kulon, M. Voysey, A. Partlow, P. Rogers, and C. Gibson, "Development of a system for anatomical landmarks localization using ultrasonic signals," in *2016 IEEE International Symposium on Medical Measurements and Applications, MeMeA 2016 - Proceedings*, 2016. DOI: 10.1109/MeMeA.2016.7533764.

[11] R. Carotenuto, M. Merenda, D. Iero, and F. G. Della Corte, "Ranging RFID Tags with Ultrasound," *IEEE Sensors Journal*, vol. 18, no. 7, pp. 29672975, 2018. DOI: 10.1109/JSEN.2018.2806564.

[12] R. Carotenuto, M. Merenda, D. Iero, and F. G. Della Corte, "An Indoor Ultrasonic System for Autonomous 3-D Positioning," *IEEE Transactions on Instrumentation and Measurement*, vol. 68, no. 7, pp. 25072518, 2019. DOI: 10.1109/TIM.2018.2866358.

[13] S. I. Lopes, J. M. N. Vieira, and D. Albuquerque, High accuracy 3D indoor positioning using broadband ultrasonic signals, in *Proc. of the 11th IEEE Int. Conference on Trust, Security and Privacy in Computing and Communications*, 2012, pp. 20082014. DOI: 10.1109/TrustCom.2012.172.

[14] A. J. Weiss and E. Weinstein, "Fundamental limitations in passive time delay estimation part I: Narrowband systems," *IEEE Transactions on Acoustics, Speech, and Signal Processing*, vol. ASSP-31, no. 2, pp. 472486, 1983. DOI: 10.1109/9780470544198.ch43.

[15] J. Zhao and Y. Wang, "Autonomous Ultrasonic Indoor Tracking System," in *2008 IEEE International Symposium on Parallel and Distributed Processing with Applications*, Sydney, NSW, 2008, pp. 532539. DOI: 10.1109/ISPA.2008.37

[16] L. Jian, Z. Yang, and Y. Liu, "Beyond triangle inequality: Sifting noisy and outlier distance measurements for localization," in *Proceedings IEEE INFOCOM*, San Diego, CA, Mar. 2010, pp. 19. DOI: 10.1109/INFCOM.2010.5462019.

[17] T. Qiao and H. Liu, "Improved least median of squares localization for non-line-of-sight mitigation," *IEEE Communications Letters*, vol. 18, no. 8, pp. 14511454, 2014. DOI: 10.1109/LCOMM.2014.2327952.

[18] J. C. Prieto, A. R. Jiménez, J. I. Guevara, J. L. Ealo, F. A. Seco, J. O. Roa, and A. D. Koutsou, "Robust regression applied to ultrasound location systems," in *IEEE PLANS, Position Location and Navigation Symposium*, 2008, pp. 671678. DOI: 10.1109/PLANS.2008.4569987.

[19] J. C. Prieto, C. Croux, and A. R. Jiménez, "RoPEUS: A new robust algorithm for static positioning in ultrasonic systems," *Sensors*, vol. 9, no. 6, pp. 42114229, 2009. DOI: 10.3390/s90604211

[20] S. Haigh, J. Kulon, A. Partlow, P. Rogers, and C. Gibson, A Robust Algorithm for Classification and Rejection of NLOS Signals in Narrowband Ultrasonic Localization Systems," *IEEE Transactions on Instrumentation and Measurement*, vol. 66, no. 3, pp. 646655, 2019. DOI: 10.1109/TIM.2018.2853878.

[21] S. Haigh, J. Kulon, A. Partlow, P. Rogers, and C. Gibson, "Mitigating the Effect of Obstacles in Narrowband Ultrasonic Localization Systems," in *IEEE International Instrumentation and Measurement Technology Conference*, Auckland, New Zealand, May 2019, pp. 15.

[22] B. Siciliano and O. Khatib, *Springer Handbook of Robotics*. Springer International Publishing, 2016.